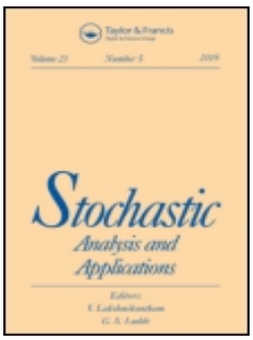

Stochastic Analysis and Applications

ISSN: 0736-2994 (Print) 1532-9356 (Online) Journal homepage: http://www.tandfonline.com/loi/lsaa20

Adaptive Estimation of FCG Using Nonlinear State-Space Models

Vassilios C. Moussas , Sokratis K. Katsikas & Demetrios G. Lainiotis

To cite this article: Vassilios C. Moussas , Sokratis K. Katsikas & Demetrios G. Lainiotis (2005) Adaptive Estimation of FCG Using Nonlinear State-Space Models, Stochastic Analysis and Applications, 23:4, 705-722, DOI: 10.1081/SAP-200064462

To link to this article: https://doi.org/10.1081/SAP-200064462

Published online: 15 Feb 2007.

Stochastic Analysis and Applications, 23: 705–722, 2005

ISSN 0736-2994 print/1532-9356 online
DOI: 10.1081/SAP-200064462

Adaptive Estimation of FCG Using Nonlinear State-Space Models

Vassilios C. Moussas
School of Technological Applications (S.T.E.F.), Technological Educational Institution (T.E.I.) of Athens, Egaleo, Greece

Sokratis K. Katsikas
Department of Information & Communication Systems, University of the Aegean, Karlovassi, Greece

Demetrios G. Lainiotis
Department of Computer Engineering & Informatics, University of Patras, Patras, Greece

Abstract: In this paper, an efficient adaptive nonlinear algorithm for estimation and identification, the so-called adaptive Lainiotis filter (ALF), is applied to the problem of fatigue crack growth (FCG) estimation, identification, and prediction of the final crack (failure). A suitable nonlinear state-space FCG model is introduced for both ALF and extended Kalman filter (EKF). Both algorithms are tested in order to compare their efficiency. Through extensive analysis and simulation, it is demonstrated that the ALF has superior performance both in FCG estimation, as well as in predicting the remaining lifetime to failure. Furthermore, it is shown that the ALF is faster and easier to implement in a parallel/distributed processing mode, and much more robust than the classic EKF.

Keywords: Adaptive algorithms; ALF; EKF; Fatigue crack growth; Failure prediction; Nonlinear FCG models; Nonlinear prediction; Stochastic models.

Received March 12, 2004; Accepted May 21, 2004
Address correspondence to Vassilios Moussas, School of Technological Applications (S.T.E.F.), Technological Educational Institution (T.E.I.) of Athens, Egaleo GR-12210, Greece; E-mail: vmouss@teiath.gr

Mathematics Subject Classification: Primary 93E10; Secondary 60G35.

1. INTRODUCTION

Fatigue crack analysis is an essential tool for life prediction and maintenance of structural components that are subjected to cyclic stresses over a prolonged period of time. Lifetime predictions and in-service inspections of each component are used to update the reliability analysis of the overall structure.

Fatigue crack growth (FCG) monitoring and failure prediction are critical in numerous engineering applications, such as civil engineering structures (e.g., bridges, multistory buildings, offshore platforms, etc.) [1]; space, aircraft, and ship applications (e.g., reusable spacecrafts, airplanes, helicopters, etc.) [2, 3]; complex and high risk plants (e.g., chemical factories, nuclear reactors, etc.) [4]; and, in general, any rare, expensive, or, dangerous structure that is impossible to test a priori in statistically large samples.

For practical applications, it is vitally important to have online, real-time monitoring and online estimation/identification of the FCG, in order to obtain earlier and more accurate predictions of remaining lifetime to failure. Any effort to attain these goals requires a) a realistic mathematical model of FCG and b) effective algorithms for accurate, fast, and efficient monitoring, estimation, and accurate prediction of FCG and the residual lifetime.

In the past, several models of the mechanism of rupture due to fatigue have been proposed. Although no complete theoretical model exists, there is a large number of semiempirical models available, of varying realism, complexity, and difficulty in their application [5, 6]. All these models are nonlinear and follow the linear elastic fracture mechanics (LEFM) concepts. Moreover, to utilize these models several methods were proposed and used with varying success, such as linear regression (LR, a standard approach for some models with a linear logarithmic form) [7, 8]; generalized least squares (GLS); nonlinear least squares (NLLS); or extended Kalman filter (EKF) (for nonlinear and more complex models) [9–11].

In this paper, an efficient adaptive nonlinear algorithm for estimation and identification, the so-called adaptive Lainiotis filter (ALF), proposed by Lainiotis [12–16], and investigated and extensively applied to important engineering problems by Katsikas and Lainiotis [17], Lainiotis and Papaparaskeva [18], Plataniotis et al. [19], and Leros et al. [20], is applied to the problem of FCG estimation, identification, and prediction of the final crack (failure). First, a stochastic nonlinear state-space model is presented, based on the most common FCG equations. Then, the presentation of the nonlinear (EKF) and adaptive

(ALF) estimation algorithms follows. Both model and methods are then tested in terms of estimation and prediction accuracy using real experimental results and with emphasis on the remaining lifetime prediction. Finally, the computational complexity efficiency of the two methods is compared. Through extensive analysis and simulation, it is demonstrated that the ALF has far superior performance both in FCG estimation, as well as in predicting the remaining lifetime to failure. Furthermore, it is shown that the ALF is faster, easier to implement in a parallel/distributed processing mode, and much more robust than the classic EKF.

2. STATE-SPACE FCG MODEL

2.1. Physical Aspects of the Model: FCG Laws

A large number of FCG models are available in the literature. Although some Markovian [21] or ARMA [22] models have been investigated, too, most of the FCG models are semiempirical deterministic laws of the form:

$$da/dN = g(a, C, n, \Delta S, \ldots) \tag{1}$$

where, a is the crack length, N the number of fatigue cycles, and $g(a)$ a nonlinear function of the crack size a and the material or loading parameters (e.g., Shanley, Paris, Forman, Larsen-Yang equations, etc.) [5, 6]. In this work, we concentrate on the simpler but widely used laws of Shanley and Paris. The nonlinear function $g(a)$ of these FCG laws is of the form:

$$g(a) = Ca^n \quad \text{(Shanley)} \tag{2a}$$

$$g(a) = C[\Delta K(a)]^n = C[\Delta S(\pi a)^{1/2} Y]^n, \quad \text{(Paris)} \tag{2b}$$

where ΔS is the loading range, Y is a function of the geometry, and C and n are material parameters to be identified. Equations (2a and 2b) are simple, general, and their logarithmic form (3a and 3b) is linear as most standard approaches require.

$$\log\left(\frac{da}{dN}\right) = \log C + n\log(a) \tag{3a}$$

$$\log\left(\frac{da}{dN}\right) = \log C + n\log(\Delta K(a)) \tag{3b}$$

Both equations can be easily integrated, and, in addition, using a simple transformation, the Shanley equation becomes identical to the

Paris equation for infinite plates (Paris-IP). For these reasons, this form of FCG law (Shanley or Paris-IP) is finally selected to demonstrate the capabilities of the nonlinear and adaptive algorithms even with less accurate models. As suggested by [23, 24], parameter estimation of the FCG laws should be performed using the crack length a as the independent variable instead of N. Equations (1 and 2) can then be written in a recursive form, provided that step Δa is sufficiently small:

$$\begin{aligned} \Delta a/\Delta N &= g(a, C, n, \ldots), \text{ or, at point } k,\ \Delta a_k/\Delta N_k = g(a_k, C, n, \ldots) \\ &\Rightarrow N_{k+1} - N_k = \Delta a / g(a_k, C, n, \ldots) \\ &\Rightarrow N_{k+1} = N_k + f_R(a_k, \Delta a_k, C, n, \ldots) \end{aligned} \tag{4}$$

All experimental results show that the crack propagation is a stochastic phenomenon [27, 28]. In order to describe the stochastic nature of FCG, these semi-empirical and deterministic FCG laws are enhanced by randomizing their parameters (e.g., C and n) or by adding some uncertainty terms, or both.

2.2. The Nonlinear State-Space Model

The model used in this work is a recursive state-space model of the form:

$$\begin{aligned} x_{k+1} &= f[k, x_k] + g[k, x_k] w_k \\ z_k &= h[k, x_k] + v_k \end{aligned} \tag{5}$$

This model is suitable for all advanced algorithms, such as EKF and ALF, and is created by the state-space representation of the general equation (4) and therefore is compatible with all semiempirical laws of type (1) [25]. In detail, the state and measurement equations are:

$$x_{k+1} = f(x_k) + w_k : \begin{bmatrix} N \\ a \\ \Delta a \end{bmatrix}_{k+1} = \begin{bmatrix} N + f\,(a, \Delta a) \\ a + \Delta a \\ \Delta a \end{bmatrix}_k + \begin{bmatrix} w_N \\ w_a \\ w_{\Delta a} \end{bmatrix}_k \tag{6}$$

$$z_k = H \cdot x_k + v_k : [N]_k = [\,1\ 0\ 0\,] \cdot \begin{bmatrix} N \\ a \\ \Delta a \end{bmatrix}_k + [v_N]_k \tag{7}$$

2.3. Augmentation of the Model

For the parameter identification problem, let θ be the vector containing all the unknown or varying parameters, then the augmented state of the model will be

$$x_\theta(k) = [x(k)|\theta]^T$$

The model equations become:

$$\begin{aligned} x(k+1) &= f[k, x_\theta(k)] + g[k, x_\theta(k)] \cdot w(k) \\ z(k) &= h[k, x_\theta(k)] + v(k) \end{aligned} \tag{8}$$

Even if the original model was linear, the augmented model becomes nonlinear and is identical to the model of eq. (5). The nonlinear state space FCG model shown in (6) and (7) is flexible and able to include and identify any number of unknown parameters in collaboration with the EKF and ALF algorithms. By augmenting its state vector with the unknown parameters vector, e.g., $\theta = [C \quad n]$, the model becomes:

$$x_{k+1} = f(x_k) + w_k : \begin{bmatrix} N \\ a \\ \Delta\alpha \\ C \\ n \end{bmatrix}_{k+1} = \begin{bmatrix} N + f_R(a, \Delta a, C, n) \\ a + \Delta a \\ \Delta a \\ C \\ n \end{bmatrix}_k + \begin{bmatrix} w_N \\ w_a \\ w_{\Delta a} \\ w_C \\ w_n \end{bmatrix}_k \tag{9}$$

$$z_k = H \cdot x_k + v_k : [N]_k = [\,1\ 0\ 0\ 0\ 0\,] \cdot \begin{bmatrix} N \\ a \\ \Delta\alpha \\ C \\ n \end{bmatrix}_k + [v_N]_k \tag{10}$$

This model is also applicable to controlled FCG experiments where Δa, N, and a are either controlled or directly observed. If an indirect non destructive testing/evaluation (NDT/NDE) method is used (e.g., acoustic emission, thermal emission, potential drop, etc.), matrix H must be replaced accordingly.

In order to apply the nonlinear method (EKF), it is also necessary to calculate the partial derivatives of the nonlinear quantities. For this state equation, matrix F contains the partial derivatives required:

$$F = \begin{bmatrix} 1 & \frac{\partial f_R}{\partial a} & \frac{\partial f_R}{\partial \Delta a} & \frac{\partial f_R}{\partial C} & \frac{\partial f_R}{\partial n} \\ 0 & 1 & 1 & 0 & 0 \\ 0 & 0 & 1 & 0 & 0 \\ 0 & 0 & 0 & 1 & 0 \\ 0 & 0 & 0 & 0 & 1 \end{bmatrix} \tag{11}$$

2.4. Statistics of the Model

In this nonlinear model, the stochastic nature of FCG is expressed by the state input vector w, the initial state vector x_0, and the measurement

error vector v. Vectors x_0, w, and v are Gaussian random variables with variances p_0, Q, and R, respectively:

$$x_0 = \begin{bmatrix} N_0 \\ a_0 \\ \Delta a_0 \\ C_0 \\ n_0 \end{bmatrix}, \; p_0 = \begin{bmatrix} p_N & 0 & 0 & 0 & 0 \\ 0 & p_a & 0 & 0 & 0 \\ 0 & 0 & p_{\Delta a} & 0 & 0 \\ 0 & 0 & 0 & p_C & 0 \\ 0 & 0 & 0 & 0 & p_n \end{bmatrix},$$
$$Q = \begin{bmatrix} q_N & 0 & 0 & 0 & 0 \\ 0 & q_a & 0 & 0 & 0 \\ 0 & 0 & q_{\Delta a} & 0 & 0 \\ 0 & 0 & 0 & q_C & 0 \\ 0 & 0 & 0 & 0 & q_n \end{bmatrix}, \; R = [R_N] \tag{12}$$

The state augmentation is necessary for parameter identification, but also presents some difficulties to the applied algorithms. i.e., i) an even higher dimensionality with higher computational requirements, ii) a higher model complexity and higher nonlinearity, and iii) more reasons to diverge leading to reduced robustness. Although EKF is susceptible to those difficulties, ALF overcomes all of them easily.

3. THE EKF

3.1. The EKF Algorithm

We consider the nonlinear model of equation (8). By taking the first terms of the Taylor expansion of the nonlinear quantities, we have:

$$\begin{aligned} f[k, x(k)] &= f[k, \hat{x}(k/k)] + F(k) \cdot [x(k) - \hat{x}(k/k)] + \cdots \\ g[k, x(k)] &= g[k, \hat{x}(k/k)] + \cdots = G(k) + \cdots \\ h[k, x(k)] &= h[k, \hat{x}(k/k-1)] + H(k) \cdot [x(k) - \hat{x}(k/k-1)] + \cdots, \end{aligned} \tag{13}$$

where

$$F(k) = \left.\frac{\partial f(k, x)}{\partial x}\right|_{x=\hat{x}(k/k)}, H(k) = \left.\frac{\partial h(k, x)}{\partial x}\right|_{x=\hat{x}(k/k-1)}, G(k) = g[k, \hat{x}(k/k)] \tag{14}$$

A linear approximation of the original model is then given by:

$$\begin{aligned} x(k+1) &= F(k) \cdot x(k) + G(k) \cdot w(k) + a(k) \\ z(k) &= H(k) \cdot x(k) + v(k) + b(k), \end{aligned} \tag{15}$$

where

$$a(k) = f[k, \hat{x}(k/k)] - F(k)\hat{x}(k/k) \quad \text{and}$$
$$b(k) = h[k, \hat{x}(k/k-1)] - H(k)\hat{x}(k/k-1) \tag{16}$$

The first-order EKF algorithm for the nonlinear model is a variation of the basic Kalman algorithm designed for the mentioned approximation [26] and is given by the following equations:

$$\begin{aligned} P(k/k-1) &= F(k) \cdot P(k-1/k-1) \cdot F^T(k) + G(k) \cdot Q(k) \cdot G^T(k) \\ K(k) &= P(k/k-1) \cdot H^T(k) \cdot [H(k) \cdot P(k/k-1) \cdot H^T(k) + R(k)]^{-1} \\ P(k/k) &= [I - K(k) \cdot H(k)] \cdot P(k/k-1) \\ \hat{x}(k/k-1) &= f[k-1, \hat{x}(k-1/k-1)] \\ \tilde{z}(k/k-1) &= z(k) - h[k, \hat{x}(k/k-1)] \\ \hat{x}(k/k) &= \hat{x}(k/k-1) + K(k) \cdot \tilde{z}(k/k-1) \end{aligned} \tag{17}$$

3.2. Necessary Augmentation and Resulting Consequences

When dealing with augmented models, the different dimensionality can create some problems for EKF that should be investigated. The model matrices are larger and more complex. A linear or trivially nonlinear model becomes highly nonlinear. More reasons for divergence appear and the robustness of the algorithm becomes questionable. Extensive tests, with Monte Carlo runs and various conditions, are required to successfully tune the algorithm to the investigated problem.

4. THE ALF ADAPTIVE EFFICIENT FCG ALGORITHM

4.1. The ALF Algorithm

We consider the model with unknown parameters shown in equation (8), but without augmenting the state by the vector θ.

$$\begin{aligned} x(k+1) &= f[k, x(k); \theta] + g[k, x(k)] \cdot w(k) \\ z(k) &= h[k, x(k); \theta] + v(k) \end{aligned} \tag{18}$$

In this model, θ is a random variable with known a-priori probability density $p(\theta/0)$.

Given the measurement set $Z_k = \{z(1), z(2), \ldots, z(k)\}$, the optimal estimation $\hat{x}(k/k)$ and the variance $P(k/k)$ are:

$$\begin{aligned} \hat{x}(k/k) &= \int \hat{x}(k/k;\theta)p(\theta/k)d\theta \\ P(k/k) &= \int [P(k/k;\theta) + \|\hat{x}(k/k) - \hat{x}(k/k;\theta)\|^2] \cdot p(\theta/k)d\theta, \end{aligned} \tag{19}$$

where $\hat{x}(k/k;\theta)$ $\kappa\alpha\iota$ $P(k/k;\theta)$ can be calculated using a Kalman filter designed for each model with parameter θ. The posteriori probability density $p(\theta/k, 0)$ of θ, given the measurements Z_k is:

$$p(\theta/k) = \frac{L(k/k;\theta)}{\int L(k/k;\theta) \cdot p(\theta/k-1)d\theta} \cdot p(\theta/k-1), \tag{20}$$

where

$$\begin{aligned} L(k/k;\theta) &= |P_{\tilde{z}}(k/k-1;\theta)|^{-1/2} e^{-1/2\|\tilde{z}(k/k-1;\theta)\|^2 \cdot P_{\tilde{z}}^{-1}(k/k-1;\theta)} \\ P_{\tilde{z}}(k/k-1;\theta) &= H(k,\theta) \cdot P(k/k-1;\theta) \cdot H^T(k,\theta) + R(k) \\ \tilde{z}(k/k-1;\theta) &= z(k) - H(k,\theta) \cdot F(k/k-1;\theta) \cdot \hat{x}(k-1/k-1;\theta) \end{aligned} \tag{21}$$

For discrete or discritized parameters, the integrals are replaced by sums and we have:

$$\hat{x}(k/k) = \sum_{i=1}^{M} \hat{x}_i(k/k)p(\theta_i/k) \tag{22}$$

$$P(k/k) = \sum_{i=1}^{M} [P_i(k/k) + \|\hat{x}(k/k) - \hat{x}_i(k/k)\|^2]p(\theta_i/k)$$

$$p(\theta_i/k) = \frac{L_i(k/k)}{\sum_{j=1}^{M} L_j(k/k) \cdot p(\theta_j/k-1)} \cdot p(\theta_i/k-1) \tag{23}$$

$$L_i(k/k) = |P_{\tilde{z}_i}(k/k-1)|^{-1/2} e^{-1/2\|\tilde{z}_i(k/k-1)\|^2 \cdot P_{\tilde{z}_i}^{-1}(k/k-1)}, \tag{24}$$

where index i indicates the quantity corresponding to the value θ_i of array θ.

4.2. Advantages/Properties

The previously presented adaptive Lainiotis filter (ALF) possesses several interesting properties:

1. Its structure is a natural parallel distributed processing architecture and hence it is more suitable to current computers clusters (see Figure 1).
2. By breaking a large nonlinear model into smaller subcases, the algorithm has a much smaller dimensionality and hence much less architectural complexity.

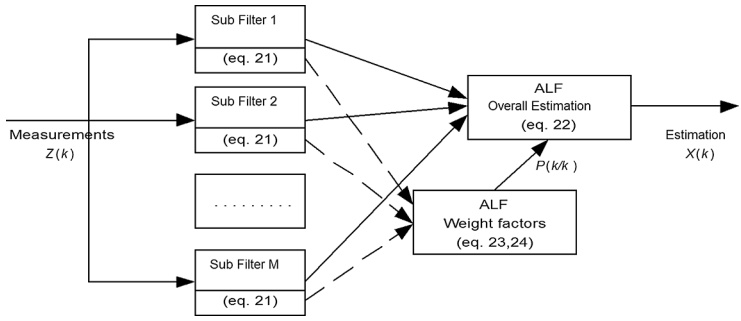

Figure 1. Subfilter parallel structure of the adaptive Lainiotis filter (ALF).

3. Although computationally intensive, it works faster due to parallelism and hence it is much more appropriate for real-time applications.
4. It is more robust than any single filter as it is capable to isolate any diverging subfilter. This is also shown by numerous applications and simulations in the literature.
5. The algorithm is well structured and modular and it is easy to implement and modify on any standard programming environment (e.g., MATLAB).

5. EXPERIMENTAL RESULTS

5.1. The Experimental Data

The experimental results of Virkler et al. [27], shown in Figure 2a, have been selected for consideration. The specimens used to obtain these results were center-cracked panels of 2024-T3 aluminum alloy 2.54 mm thick, 558.8 mm long, and 152.4 mm wide. The total number of specimens was 68. The load was of sinusoidal form with frequency 20 Hz, maximum value $P_{max} = 23.353$ kN, and load ratio $R = 0.20$. Data recording started at crack length, a, of 9 mm and extended to a final length of 49.80 mm. The accumulated number of cycles was recorded for each $\Delta a = 0.20$ mm, first, and it was increased to 0.40 and to 0.80 mm after crack lengths of 36.20 mm and 44.20 mm, respectively. Thus, each specimen produced 165 data points.

5.1.1. Data Curves Representation and Fitting

Clearly, due to the mode of recording, these data are not equidistant in time (= number of cycles) as the current analysis requires. With the objective of preserving the raw data, the way to overcome this minor

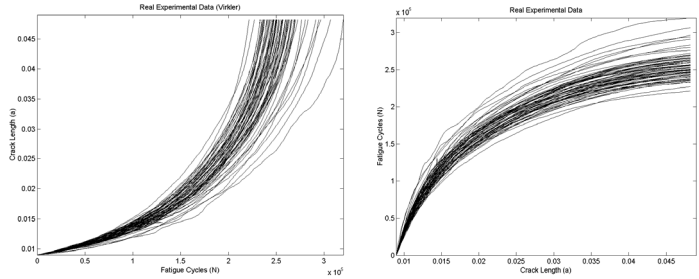

(a) (b)

Figure 2. Crack growth histories from 68 specimens; (a) original (α vs. N) and (b) modified (N vs. α) presentation of the crack growth curves.

problem is by switching the roles of the variables (Figure 2b), i.e., by considering the crack size a as the independent variable ("time") and the number of cycles N as the dependent variable to be studied (number of cycles to failure = lifetime). This point of view is in full accord with [23] and [28].

The experimental curves were first treated using simple methods that produced some average estimation of the model parameters. Using the Shanley law and the LR and NLLS, we estimated the mean parameter values for the entire set of the 68 curves, as well as for each curve separately (Table 1). These estimations can be used either as initial values or as reference values. We can also consider those mean values as our a priori knowledge and calculate the a priori predictions of the expected lifetime, i.e., before any new data become available.

In the "C only" case, parameter n is considered known and equal to its mean value for all 68 curves and only parameter C was calculated.

Table 1. Mean parameter values estimated by the LR and NLLS methods

Model (Method)	Experim. data	Estimated parameters	No. of values	Mean	Variance
Shanley logarithmic (LR)	Cloud of ~11,000 points	n	1	1.86009	–
		C	1	0.000204618	–
		C only	~11,000	0.000211324	3.2901e−09
Shanley recursive (NLLS)	Set of 68 curves	n	68	1.8091	1.3165e−02
		C	68	0.00018194	1.1324e−08
		C only	68	0.00016176	1.1644e−10

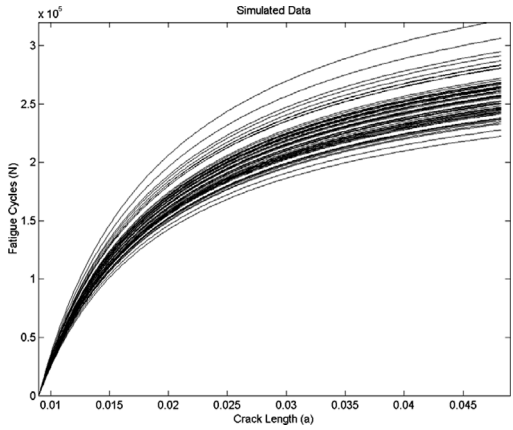

Figure 3. Simulated data sets recreated using Shanley law and parameter C values from Table 1.

Using Shanley law and parameter C estimations from Table 1 (last case), we recreate 68 "ideal" curves. The simulations, as shown in Figure 3, represent well the stochastic nature of FCG, although they are smooth and do not cross each other. Depending on the selected FCG law and the unknown parameters, we can produce more sets of simulated data (with varying accuracy), but in this work we focus on the estimation algorithms and their capabilities, so we considered only the simple Shanley and Paris-IP laws.

5.1.2. Simulation and Lifetime Prediction

In online real time cases, reception and treating of additional data improves the final predictions. When we start early with fewer points, our predictions are not so accurate. After the middle point, the predictions become more accurate and get closer to the real values. Depending on the starting point along the crack propagation curve, the prediction of the final crack size and its confidence (variance) vary significantly (Figure 4).

Later in our analysis, the final crack is repeatedly predicted at each estimated point, and thus producing a continuous curve indicating the progress of lifetime prediction. For comparison reasons, we also use three thresholds or prediction points (Figure 4) that correspond approximately to the 5%, 20%, and 50% of a curves data. Finally, in our tests, we often consider the worst case scenario, using experiments as far as possible from the average. Such experiments are the two early or leftmost (15, 64) and the two late or rightmost (49, 37) curves.

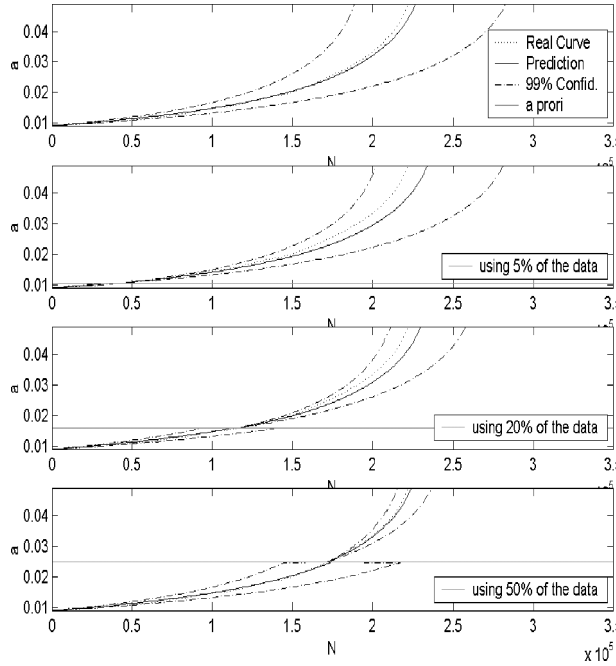

Figure 4. Simulation of the 15th curve and prediction of the final crack size from four different starting points: without data (a-priori) and from the 9th, 36th, and 80th points of the curve.

5.2. Estimation Using the Nonlinear and Adaptive Algorithms

5.2.1. The EKF Nonlinear Estimator

The EKF nonlinear estimator, shown in equation 17, is applied to the crack growth experimental data of Figure 2b, using the nonlinear and augmented state space model (equations 9–10) for Shanley law. Parameter n is considered known, constant, and equal to its mean value. Parameter C is considered unknown and therefore it is included in the augmented state for estimation with initial mean and variance $\{C_0, p_C\}$. The results of the experimental data analysis in Table 1 are used as initial values and statistics of the filter. State and measurement statistics were calculated by comparing the real data (Figure 2b) to the "ideally" simulated ones (Figure 3) by the Shanley crack law.

5.2.2. The ALF Adaptive Estimator

The ALF adaptive estimator shown in equations 19–24 is also applied using the nonlinear state space model of equations 6–7, to the crack

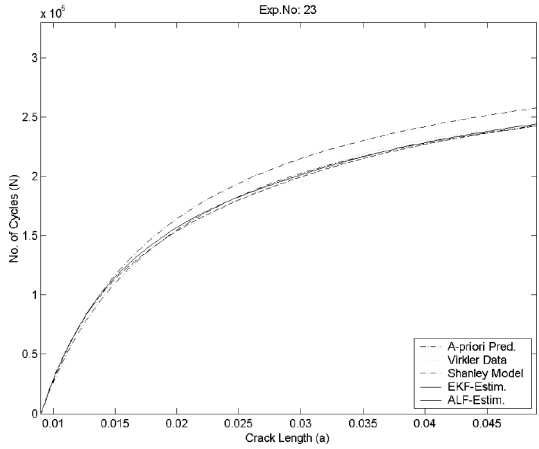

Figure 5. EKF and ALF estimations for a single experiment.

growth experimental data of Figure 2b, and with the same initial values and statistics. The ALF, instead of state augmentation, uses a number of EKF estimators with their corresponding nonlinear models. Each estimator uses the nonlinear model with a different value for the C parameter. All possible values are within the area defined by the results in Table 1. The optimal number of these filters depends on the specific case under consideration. In our case, we obtained excellent results using just five to seven nonlinear filters.

Before applying any estimation algorithm, we also calculate the a-priori prediction based on the average values estimated by the standard LR and the NLLS methods (Table 1). Figure 5 presents the real and simulated data, the a-priori prediction, and the EKF and ALF estimations for one experimental curve. The EKF and ALF estimation errors for the same curve become clearer in Figure 6a.

5.3. Prediction Using the Nonlinear and Adaptive Algorithms

As explained earlier (Figure 5), we also perform a remaining life prediction at each data point, in order to calculate the number of fatigue cycles (N) required for the crack length (a) to reach a critical final size. The prediction is usually improved as more data points become available.

Figure 6b presents the EKF and ALF prediction errors for the same experiment. The vertical lines represent the amount of data used (5%, 20%, and 50%). Prediction errors start from the a-priori error and gradually converge to 0, i.e., the correct number of fatigue cycles.

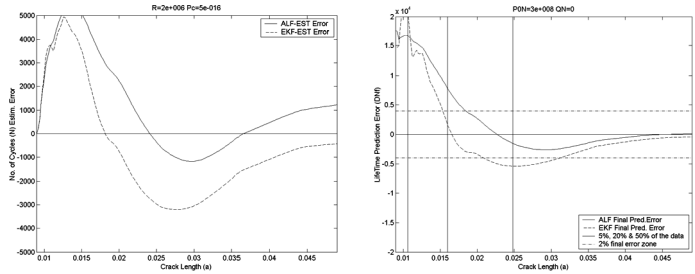

(a) (b)

Figure 6. EKF and ALF estimation errors (a) and prediction errors (b) for a single experiment.

The horizontal lines represent a prediction accuracy threshold equal to $\pm 2\%$ of the correct value. For the specific experiment in Figure 6b, we see that ALF reaches the 2% threshold much earlier having received only 30% of the data, when EKF needs more than 60% of the data to reach the same accuracy.

As the results from single experiments vary significantly, most comparisons are made by averaging the results from five to ten experiments. The smoother curves represent better the mean behavior of the EKF and ALF algorithms. Figure 7 presents the average prediction errors for EKF and ALF. Clearly, the ALF crosses the 2% error limit with less than 20% of the data. EKF crosses the same limit much later, using more than 50% of the data.

5.4. Number of Filters: Accuracy and Complexity

The number of filters used by ALF affects directly the accuracy and the complexity of the algorithm. In Figure 7, in addition to the ALF with 7 filters, two more implementations are shown: a simpler ALF using 3 filters and a heavier ALF with 18 filters. Using more filters, their in between distance becomes smaller and the ALF performance improves. After a certain number of filters, the performance improvement is very small in comparison to the increased complexity. In our case, the use of 7 subfilters proved to be an optimal implementation for ALF.

The robustness of ALF is also improved with the increased number of EKF subfilters. EKF is sometimes diverging due to errors or mistuning. This is fatal when a single EKF is applied for estimation, as there are no means to correct it. This is not a problem in ALF as it includes the mechanism to discard any EKF that is not performing satisfactorily. If an EKF subfilter diverges, its a posteriori probability tends to zero and its results are ignored. This behavior guaranties the

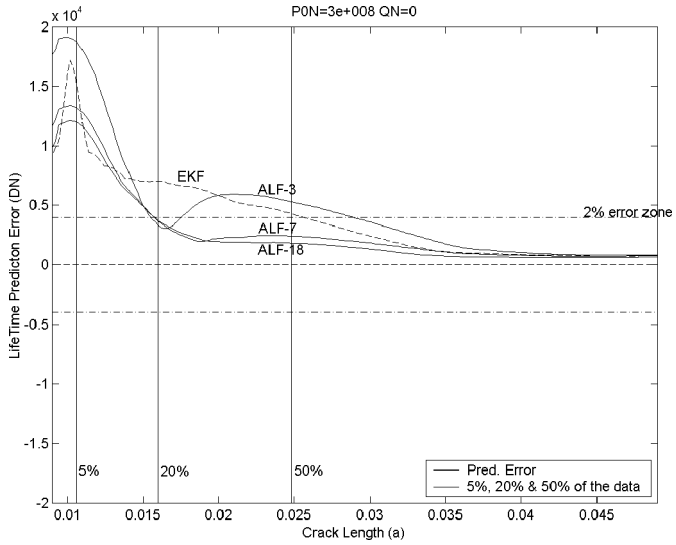

Figure 7. EKF and ALF average prediction errors over ten experiments. The three ALF implementations shown, use 3, 7, and 18 filters, respectively.

increased ALF robustness against any subfilter failure or any single EKF estimator.

The advanced ALF algorithms are more complex and require more operations and, normally, they are more time consuming. Detailed analysis of the computational requirements for EKF and ALF can be found in [29], where it is shown that the complexity and the time consumption depends on the problem dimensionality and on the partitioning capabilities of the algorithm. It is also shown that parallel implementation is essential for the ALF algorithm. The internal structure of ALF is suitable for parallel implementation as all subfilters are decoupled and can be implemented by separate processors. As a result, the total number of operations may be higher but the time requirements are dramatically reduced to those of a single EKF filter plus a small overhead for the ALF equations (22–24).

Based on this analysis, a number of EKF and ALF implementations were analyzed for the state-space model of equations 6–7. For each case studied, the required operations per iteration are calculated and shown in Figure 8.

The EKF time requirements increase exponentially when its state is augmented by 1 to 4 parameters. The ALF time requirements also increase with the number of EKF subfilters, but only when the filter is implemented sequentially. If ALF is implemented in parallel, the time requirements are minimal and the filter overhead increases linearly.

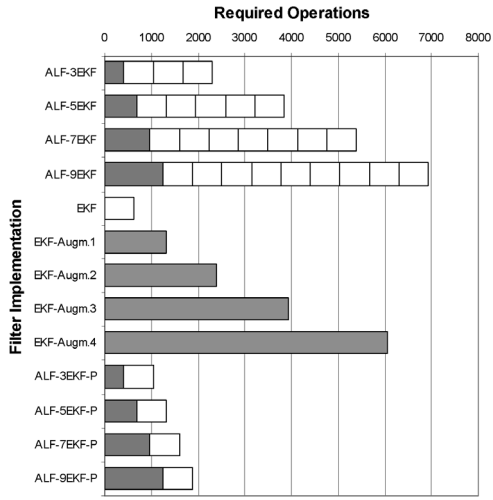

Figure 8. Computational requirements comparison for EKF, ALF, and ALF in parallel implementation.

The EKF requirements (without augmentation, as it used by ALF) are also shown for reference.

5.5. Remarks on ALF Efficiency

1. Note that the proposed adaptive nonlinear ALF predicts the actual time to failure much sooner than the EKF, using less than half of the measurements that EKF requires.
2. Note also that both nonlinear predictors do converge to the actual time. However, the ALF does so much sooner than EKF and with fewer measurements, i.e., computations.
3. In other words, use of the ALF gives: a) better time to failure prediction, much sooner (in time for corrective action); b) it does so with fewer required measurements (and hence far less data acquisition cost); and c) the ALF using fewer measurements requires a much fewer number of computations (reduced computational cost).

6. CONCLUSIONS

The adaptive nonlinear algorithm ALF is applied to the FCG problem for estimation and residual lifetime prediction. The ALF is tested against a classic EKF with augmented state. Both filters use a nonlinear state-space representation of a simple FCG law, and real experimental data.

The results show that both predictors do converge to the actual time to live. However, ALF can do it more accurately and much sooner than the EKF. More precisely, ALF converges sooner to the correct predictions requiring fewer measurements, and leaving more time for reaction, than the EKF. Due to its partitioned structure, ALF is suitable for parallel implementation. Parallel ALF overcomes easily its complexity as it performs faster than the corresponding EKF. In addition, ALF is more robust than a single EKF as it incorporates the mechanism to isolate any diverging subfilter.

REFERENCES

1. Madsen, H. O., R. K. Skjong, and F. Kirkemo. 1987. Probabilistic FCG analysis of offshore structures with reliability updating through inspection. In *Proceedings of the Marine Structural Reliability Symposium*, Arlington, Verginia, USA, October 1987. Society of Naval Architects and Marine Engineers.
2. Sutharshana, S., M. Creager D. Ebbeler, and N. Moore. 1992. A probabilistic fracture mechanics approach for structural reliability assessment of space flight systems. In *Advances in Fatigue Lifetime Predictive Techniques: Proceedings of the Symposium*, pages 234–246. San Francisco, California, USA, April 1990. American Society for Testing and Materials.
3. Newman, J. C., Jr. 1981. A crack closure model for predicting fatigue crack growth under aircraft spectrum loading. *ASTM STP* 748:53–84.
4. Lucia, A. C. 1985. Probabilistic structural reliability of PWR pressure vessels. *Nucl. Eng. Design* 87:35–49.
5. Schutz, W. 1979. The prediction of fatigue life in the crack initiation and propagation stages: A state of the art survey. *Eng. Fract. Mech.* 11:405–421.
6. Kaminski, M. 2002. On probabilistic fatigue models for composite materials. *Int. Journal of Fatigue* 24:477–495.
7. Standard Designation E647-93 1994. *Standard Test Method for Measurement of FCG Rates*. American Society for Testing Materials 03(01):679–706.
8. Fuchs, H. O., and R.I. Stephens. 1980. *Metal Fatigue in Engineering*. New York: J. Wiley & Sons.
9. Moussas, V. C., G. Solomos, and A. C. Lucia. 1994. A general method for raw fatigue crack growth data processing and structural reliability assessment. In *Computational Stochastic Mechanics, Proceedings of the 2nd International Conference on Computational Stochastic Mechanics*, Athens, Greece, June 1994. A. A. Balkema, Roterdam, 697–703.
10. Ray, A., and S. A. Tangirala. 1997. Nonlinear stochastic model of fatigue crack dynamics. *Prob. Engng. Mech.* 12(1):33–40.
11. Patankar, R., and A. Ray. 2000. State-space modeling of fatigue crack growth in ductile alloys. *Engineering Fracture Mechanics* 66:129–151.
12. Lainiotis, D. G. 1984. Adaptive dynamic modelling, risk assessment, failure detection and correction. In *Advances in Structural Reliability, Proceedings of the Advanced Seminar on Structural Reliability*, Ispra, Italy, June 1984. Dordrecht: D. Reidel Pub Co., 165–193.

13. Lainiotis, D. G., and V. C. Moussas. 1987. Theory and application of partitioning filters for identification. In *Advances in Structural Reliability, Proceedings of the Advanced Seminar on Structural Reliability*, Ispra, Italy, May. CEC Joint Research Centre—Ispra Courses Notes ASR/87/10, 1–18.
14. Lainiotis, D. G. 1971. Optimal adaptive estimation: Structure and Parameter Adaptation. *IEEE Trans on AC* 16(2):160–169.
15. Lainiotis, D. G. 1974. Partitioned estimation algorithms, I: Nonlinear estimation. *Information Sciences* 7:203–235.
16. Lainiotis, D. G. 1976. Partitioning: A unifying framework for adaptive systems, I: Estimation. *IEEE Proceedings* 64(8):1126–1143.
17. Katsikas, S. K., and D. G. Lainiotis. 1997. Lainiotis filters applications in seismic signal processing. *Nonlinear Analysis, Theory, Methods and Applications* 30(4):2385–2395.
18. Lainiotis, D. G., and P. Papaparaskeva. 1996. Joint estimation and identification of LIDAR log power returns in a switching environment. *Applied Optics LP* 35(33):6466–6478.
19. Plataniotis, K. N., S. K. Katsikas, D. G. Lainiotis, and A. N. Venetsanopoulos. 1999. Optimal seismic deconvolution: distributed algorithms. *IEEE Trans. on Geoscience and Remote Sensing* 36(3):779–792.
20. Leros, A. K., N. V. Nikitakos, and S. K. Katsikas. 1998. Towed array shape estimation using multimodel partitioning filters. *IEEE Trans. on Oceanic Engineering* 23(4):380–384.
21. Bogdanoff, J. L., and F. Kozin. 1985. *Probabilistic Models of Cumulative damage*. New York: Wiley.
22. Solomos, G. P., and V. C. A. Moussas. 1991. Time series approach to fatigue crack propagation. *Structural Safety* 9:211–226.
23. Kozin, F., and J. L. A. Bogdanoff. 1981. Critical analysis of some probabilistic models of fatigue crack growth. *Eng. Fract. Mech.* 14:59–89.
24. Ostergaard, D. F., and B. M. Hillberry. 1983. Characterization of the variability in fatigue crack propagation data. In *Probabilistic Fracture Mechanics and Fatigue Methods: Applications for Structural Design and Maintenance*. ASTM STP 798, 97–115.
25. Moussas, V. C. 2002. *Non-Linear Estimation Algorithms in Component Lifetime Prediction for Improved Structural Safety*. PhD Dissertation; Dept. Comp. Eng., Univ. of Patras, Greece.
26. Anderson, B. D. O., and J. B. Moore. 1979. *Optimal Filtering*. New Jersey: Prentice-Hall.
27. Virkler, D. A., B. M. Hillberry, and P. K. Goel. 1979. The statistical nature of fatigue crack propagation. *Transactions of ASME J. Engineering Materials Technology* 101:148–153.
28. Ortiz, K., and A. Kiremidjian. 1986. Time series analysis of fatigue crack growth rate data. *Eng. Fract. Mech.* 24:657–675.
29. Katsikas, S. K., S. P. Likothanassis, and D. G. Lainiotis. 1991. On the parallel implementations of the Kalman and the Lainiotis filters and their efficiency. *Signal Processing* 18:289–305.